Soft Matter

PAPER

Fast responsive and morphologically robust thermo-responsive hydrogel nanofibres from poly(*N*-isopropylacrylamide) and POSS crosslinker†

Jing Wang, Alessandra Sutti, Xungai Wang and Tong Lin*

Stable thermo-responsive hydrogel nanofibres have been prepared by electrospinning of commercial poly(*N*-isopropylacrylamide) (PNIPAM) in the presence of a polyhedral oligomeric silsesquioxane (POSS) possessing eight epoxide groups and of an organic-base catalyst, followed by a heat curing treatment. The nanofibres showed excellent hydrogel characteristics with fast swelling and de-swelling responses triggered by temperature changes. They were also morphologically robust as their physical integrity was preserved upon repeated hydration/dehydration cycles and exposure to solvents.

Introduction

Hydrogels capable of responding to surrounding temperature variations by swelling and de-swelling, also called thermo-responsive hydrogels,[1] are the most studied "smart" polymeric gels. They have been widely explored for development of temperature-triggered intelligent devices with applications in areas such as drug delivery,[2] sensors,[3] actuators,[4] photonics,[5] and optics devices.[6] Depending on the chemical composition and structure, as well as on the physical construction, thermo-responsive hydrogels may show significant differences in swelling and de-swelling kinetics. The most significant challenge for thermo-responsive hydrogels has been to achieve both fast response and structural integrity during the repeated volume changes.[7] The former requires water to access the whole material rapidly. To this end, nano-structures are considered to be ideal because they are usually accompanied with increased porosity and decreased thickness in the solid domains. Indeed, thermo-responsive hydrogel nanoparticles and mesoporous membranes have been reported.[8] However, it is difficult to construct mechanically robust macrostructures by using nanoparticles alone. Mesoporous membranes, on the other hand, show slow response due to the small pore size, but good retention of morphology. In contrast to the response speed, the structural robustness, which is very relevant to the effective applications of a hydrogel, is determined by the structure of the material at both the molecular and the macroscopic levels, but has received little attention.

Nanofibres, mostly produced by electrospinning, have a large surface-to-weight (or volume) ratio, high porosity with excellent pore-interconnectivity, and are easily functionalised. This endows electrospun nanofibres with enormous potential towards several applications.[9] The nonwoven-like fibrous structure produced by electrospinning is highly desired for a thermo-responsive hydrogel to achieve fast hydration/dehydration response, because water can easily access the surface of each fibre and the small fibre diameter also increases the overall fibre surface area, facilitating the intrafibre mass exchange.

Among all thermo-responsive polymers reported, poly(*N*-isopropylacrylamide) (PNIPAM) is the most popular and has been widely studied.[10] PNIPAM shows a temperature-induced negative volume transition taking place at the lower critical solution temperature (LCST). Below LCST, the polymer is highly hydrated and swollen. When the temperature is above LCST, the polymer undergoes molecular rearrangement, resulting in dehydration and considerable shrinkage in volume (de-swelling). Linear PNIPAM is soluble in cold water, and nanofibres electrospun from linear PNIPAM are therefore unstable and not able to maintain their structural integrity in water.[11] Improvement of the wet-stability has been reported through a copolymer of PNIPAM and stearyl acrylate, where a physically crosslinked inter-polymer network is generated because of the hydrophobic interactions of stearyl side-chains.[12] However, these physically crosslinked hydrogel nanofibres have low stability in organic solvents, which restricts their applications. PNIPAM hydrogel nanofibres having a chemically crosslinked macromolecular network, thus dimensionally stable in both water and organic liquids, and a fast hydration/dehydration response have not been reported in research literatures.

In bulk, PNIPAM-based hydrogels are prepared mainly by direct co-polymerisation of *N*-isopropylacrylamide (NIPAM) with a multi-functional monomer, or by crosslinking of copolymers consisting of NIPAM and other crosslinkable moieties.[13] However, pre-crosslinked PNIPAM cannot be electrospun into

Centre for Material and Fibre Innovation, Deakin University, Geelong, VIC, 3217, Australia. E-mail: tong.lin@deakin.edu.au

† Electronic supplementary information (ESI) available: Visible transmittance, FTIR and XPS survey spectra, NMR, TG curves, XRD patterns, SEM images, elemental analysis results, crosslinking reaction mechanism, and organic solvent-induced de-swelling. See DOI: 10.1039/c1sm00010a

nanofibres because of its insoluble nature, and mixtures of small molecule monomers are not electrospinnable either. Electrospinning of linear high molecular weight PNIPAM followed by chemical crosslinking would thus be ideal to prepare stable hydrogel PNIPAM nanofibres, but has not yet been reported in research literatures.

In this paper, for the first time we report on the preparation of highly crosslinked PNIPAM hydrogel nanofibres simply by electrospinning of commercial PNIPAM in the presence of a POSS crosslinker possessing eight epoxide groups and a strong base catalyst (2-ethyl-4-methylimidazole, EMI), followed by a heat treatment. We have found that the addition of the catalyst significantly enhances the formation of a highly crosslinked polymer network, ensuring the nanofibrous structure is maintained during the curing treatment. The as-prepared hydrogel nanofibres showed not only fast swelling/de-swelling responses triggered by temperature changes, but also excellent morphological robustness after undergoing repeated hydration/dehydration cycles. POSS was used as the crosslinker because it has eight reactive epoxide groups and its silica cage endows the crosslinked polymer with a robust nanocomposite structure at the molecular level.[14]

Experimental

Materials

Poly(N-isopropylacrylamide) (M_W 300 000 Da, Polysciences), Octaglycidyl polyhedral oligomeric silsesquioxane (OpePOSS, Hybrid Plastics Inc.), 2-ethyl-4-methylimidazole (EMI, Sigma) and all other chemicals were of analytical grades. The polymer solutions for electrospinning were prepared by dissolving PNIPAM, OpePOSS and EMI in a N,N′-dimethylformamide (DMF)/tetrahydrofuran (THF) (1 : 1, vol/vol) solution at room temperature. PNIPAM concentration was 10 wt%.

Preparation of hydrogel nanofibres

Nanofibres were electrospun using a needle electrospinning setup.[15] During electrospinning, the solution flow rate, the applied voltage and the electrospinning distance were set at 0.6 ml h⁻¹, 13 kV and 17 cm, respectively. After electrospinning, the as-spun nanofibres were heated in a 160 °C vacuum oven for 4 hours (vacuum around 50 mmHg).

Characterisation

Fibre morphology was observed under a scanning electron microscope (LEO1530) and a laser scanning confocal microscope (Leica TCS SP5) equipped with Argon lasers. FTIR and UV-VIS spectra were obtained from a Bruker Vertex 70, FTIR spectrometer and an Ocean Optics Inc PX-2 UV-VIS spectrophotometer, respectively. X-Ray photoelectron spectra were collected on a VG ESCALAB 220-iXL XPS spectrometer with a monochromated Al Kα source (1486.6 eV) using samples of ca. 3 mm² in size. The X-ray beam incidence angle is 0° with respect to the surface normal, which corresponds to a sampling depth of ca. 10 nm. Differential scanning calorimetry (DSC) measurement and Thermogravimetric Analysis (TGA) were conducted on

a TA DSC Q200 instrument in a dry nitrogen atmosphere at a heating/cooling rate of 5 °C min⁻¹.

Results and discussion

To produce nanofibres, a DMF/THF (1 : 1, vol/vol) solution of PNIPAM, OpePOSS and EMI was electrospun using a conventional electrospinning setup. The morphology of the as-spun nanofibres is shown in Fig. 1a. Bead-free uniform fibres with a diameter in the range of 700–900 nm were obtained from the electrospinning process. The fibres showed a smooth surface and no preferential alignment within the fibrous membranes. The as-spun nanofibre mat started dissolving on contact with water.

To generate a highly crosslinked PNIPAM network, the as-electrospun nanofibres were subjected to a heat treatment at 160 °C for 4 hours under vacuum. After the treatment, the fibres showed very small morphological change, and the fibre diameter increased slightly from 870 ± 110 nm to about 970 ± 120 nm (Fig. 1b). To demonstrate the stability of the cured PNIPAM nanofibres, the fibres were immersed in water until they fully swelled, and the swollen nanofibres were then dried by two different methods. In one method, the fully swollen nanofibres were immersed in 40 °C water to induce de-swelling, after which the de-swollen nanofibres were vacuum dried at 40 °C. As shown in Fig. 1c, the fibres maintained their fibrous morphology after drying in this way, although the diameter became larger (average diameter, 1.8 μm). Such an increase in fibre diameter is quite common for electrospun hydrogels, and has been ascribed to the relaxation of the macromolecular network upon drying.[16] In another method, the swollen nanofibres were dried at 25 °C in vacuum, which resulted in even coarser fibres (average diameter 2.6 μm) (Fig. 1d). However, when the dried nanofibres were rehydrated, they became swollen again and the fibres changed to the respective dimensions upon drying at the different conditions.

Fig. 2a shows the appearance of the cured nanofibre mat. Like the non-cured ones, the cured nanofibres appeared white and opaque. Upon contacting with cold water (e.g. 20 °C), the cured
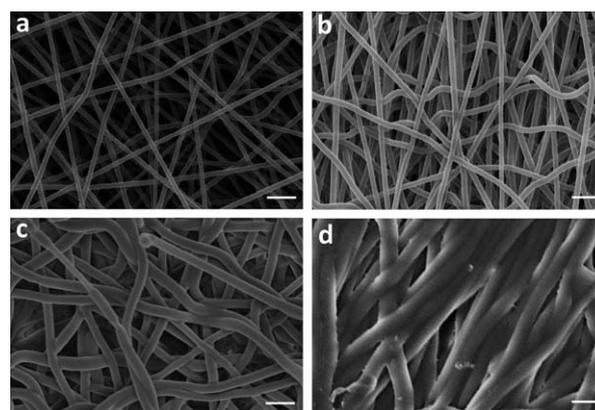
Fig. 1 SEM images of (a) non-cured nanofibres, (b) cured nanofibres, (c) cured nanofibres after swelling in 25 °C water, de-swelling at 40 °C and then drying in vacuum at the same temperature for 4 h, and (d) cured nanofibres after swelling in 25 °C water and drying in vacuum at 25 °C (4 h). (PNIPAM : OpePOSS : EMI = 100 : 15 : 0.3, w/w; scale bar: 5 μm).
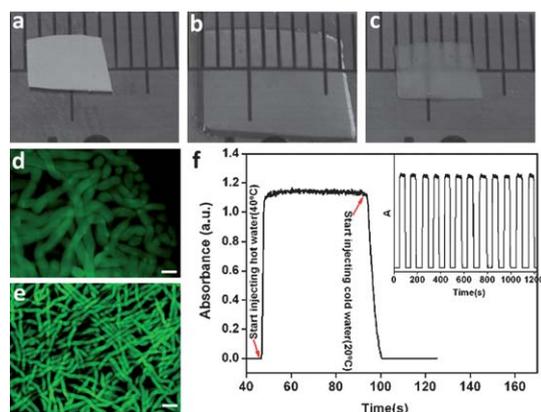
Fig. 2 (a~c) Digital images of the cured PNIPAM nanofibre membranes, a) just after curing, b) swelling in cold water (20 °C), c) swelling in cold water and then de-swelling in 40 °C water. d & e CLSM images of d) swollen PNIPAM nanofibres in cold water (20 °C), e) de-swollen fibers after introducing warm water (40 °C) (the fiber mat was dyed with fluorescein isothiocyanate before the CLSM imaging). f) Optical transmittance changes of cured nanofibre membrane in alternate cold and warm water flows (wavelength 650 nm). (PNIPAM : OpePOSS : EMI = 100 : 15 : 0.3, wt/wt; scale bar in d and e: 10 μm)

nanofibre mat rapidly became swollen (within 3 seconds) and highly transparent (Fig. 2b). This swollen nanofibre mat was very flexible, although it was highly stable in dimensions. The fibre mat showed no degradation and weight change after immersion in cold water for 4 weeks. Based on the weight changes, the swelling ratio of the nanofibre can be calculated as, $Q = (W_w - W_d)/W_d$, where W_w and W_d are the weight of the wet and the dry samples, respectively. The maximum swelling ratio was measured to be 23.0. It should be noted that Q is inclusive of all water that is absorbed within the nanofibre and in the inter-fibre space because of the highly porous nanofibrous structure. Since the volume transition of PNIPAM is isotropic, the swelling or de-swelling of the nanofibres should involve changes in both diameter and length.

When the swollen cured nanofibres were heated to 40 °C, they responded to the temperature change within seconds. The de-swelling process, which took place at 40 °C, reduced the transparency and the dimensions of the nanofibre membrane, while preserving its actual shape (Fig. 2c). Such an expansion and contraction can be repeated reversibly for many times.

The swollen and de-swollen hydrogel fibres were also observed through confocal laser scanning microscopy (CLSM). A fluorescent-dye-stained nanofibre mat was repeatedly immersed in 20 °C and 40 °C water baths. The typical fibre morphologies are shown in Fig. 2d and e. Upon immersing in the colder water, the average fibre diameter increased up to 9 μm. However, when the fully swollen fibres were put into 40 °C water, the average diameter decreased to about 3 μm.

Since swelling and de-swelling involved a change in the transparency of the fibre samples, the temperature dependence of optical transmittance was measured, and showed sensitive to temperature changes ranging between 30 °C and 32 °C (ESI†), which corresponded to a relative volume change between 0.15 and 0.70 (based on the fully swollen state, ESI†). The optical

transmittance of the nanofibre mat was used to examine the thermo-responsive speed. To do this, a nanofibre mat was immobilised in an enclosed cuvette, in which cold (20 °C) and warm (40 °C) water were alternatively introduced. An optical fibre UV-VIS spectrophotometer was used to monitor the transmittance change (see ESI†). Fig. 2f shows the typical temperature response curve. The nanofibre mat responded very quickly to the temperature changes. Within 2 seconds from feeding 40 °C water, the sample transmittance reached a minimum value, and within 3 seconds from introducing the colder water, the nanofibre membrane became completely transparent. Upon alternatively introducing the warmer and the colder water, the transmittance of the fibrous membrane changed reproducibly. The swelling and de-swelling cycle was repeated at least 50 times without degradation of the sample or of its performance.

For comparison, PNIPAM/OpePOSS nanofibres without EMI were also electrospun. The as-spun nanofibre mats showed apparent shrinkage during the curing thermal treatment. The shrinkage became much more serious when the treatment was performed at 180 °C, a condition similar to what reported in literature for the preparation of PNIPAM/OpePOSS bulk hydrogels.[17] Fig. 3 shows the shrinkage of these samples. SEM images reveal that the diameter of the fibres which do not contain EMI increases considerably after the heat treatment at 160 °C (Fig. 3b″). For the samples treated at 180 °C, no fibres can be
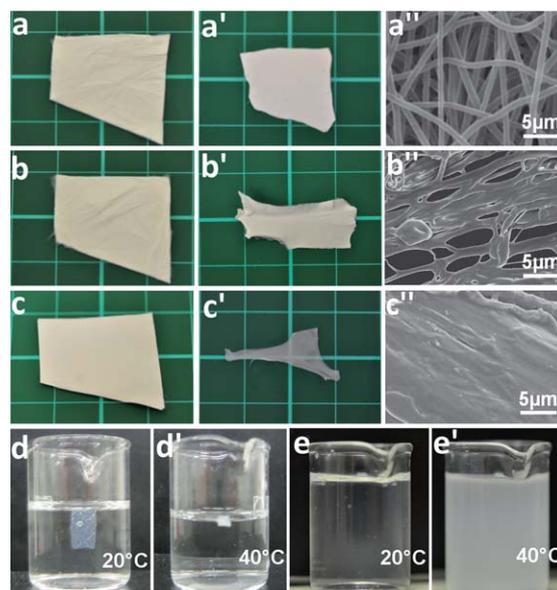
Fig. 3 (a and a′) PNIPAM/OpePOSS/EMI nanofibres before and after heat treatment at 160 °C for 4 h (PNIPAM : OpePOSS : EMI = 100 : 15 : 0.3, w/w). (b and b′) PNIPAM/OpePOSS nanofibres without EMI before and after heat treatment at 160 °C for 4 h (PNIPAM : OpePOSS = 100 : 15, w/w). (c and c′) PNIPAM/OpePOSS nanofibres without EMI before and after heat treatment at 180 °C for 4 h (PNIPAM : OpePOSS = 100 : 15, w/w). (a″–c″) SEM images of the nanofibres after the respective heat treatments. (d and d′) Cured PNIPAM/OpePOSS/EMI nanofibres in 20 °C and 40 °C water. (e and e′) PNIPAM/OpePOSS nanofibres without EMI after curing at 160 °C for 4 h, (e) immersed in 20 °C water for 20 min, and then (e′) the same heated to 40 °C.

identified from the SEM image (Fig. 3c″). Moreover, after the treatment, when the fibres containing no EMI were immersed in cold water, they dissolved completely, and no fibrous structure was recovered when the water was heated to 40 °C (Fig. 3e and e′). This result suggests that the crosslinking in the absence of EMI at temperatures below 180 °C is of very low efficiency and that the treated fibres show no hydrogel characteristics, dissolving upon contact with water.

Besides being stable in water, the cured PNIPAM/OpePOSS/EMI nanofibres were also stable in organic solvents. It was interesting to find that when a water-miscible solvent (e.g. ethanol and acetone) was dropped on a water-swollen hydrogel fibre mat, the fibre mat dehydrated rapidly, but still maintained the actual shape (see ESI†). Such a water-swelling/solvent de-swelling cycle is reversible and can be repeated many times.

The repeatable swelling/de-swelling behaviour and the morphological robustness of the cured hydrogel fibres were attributed to the crosslinked polymer network formed within the fibres. Scheme 1 illustrates the suggested crosslinking reaction, which takes place during the curing treatment of the nanofibres. In chemistry, the H–N in the isopropylacrylamide has a very low reactivity, even towards epoxide groups.[18] However, when the reaction was catalysed by a strong base, imidazole for instance, the reaction between H–N and epoxide group was enhanced, resulting in improved crosslinking efficiency. A mechanism for the catalysed chemical reaction between the NIPAM unit and OpePOSS was proposed and shown in the ESI†.

The crosslinking reaction was confirmed by FTIR, XPS, elemental analysis, DSC and NMR tests. After the curing treatment, the epoxide characteristic peaks at around 840 cm⁻¹ and 910 cm⁻¹ in the FTIR spectrum disappeared (see ESI†), confirming the ring-opening of the epoxide groups in OpePOSS. Curve-fitting of the high resolution N1s XPS spectra revealed that a peak with the binding energy of 400.3 eV appeared after the curing treatment, corresponding to O=C–N–C(C) groups,[19] besides the main peak at 399.6 eV for O=C–N–C(H) (Fig. 4a and b). According to the peak area, the N-atoms participating in the crosslinking reaction can be calculated to be 8.25% when 15% OpePOSS (based on the PNIPAM by weight) was used. This value is close to the theoretical value (10.1%) calculated according to the actual weights of OpePOSS and PNIPAM used for electrospinning.

To verify the crosslinking reaction, the cured nanofibres were also subjected to a harsh leaching treatment with both water and
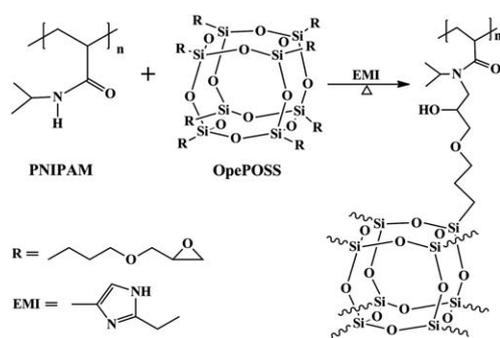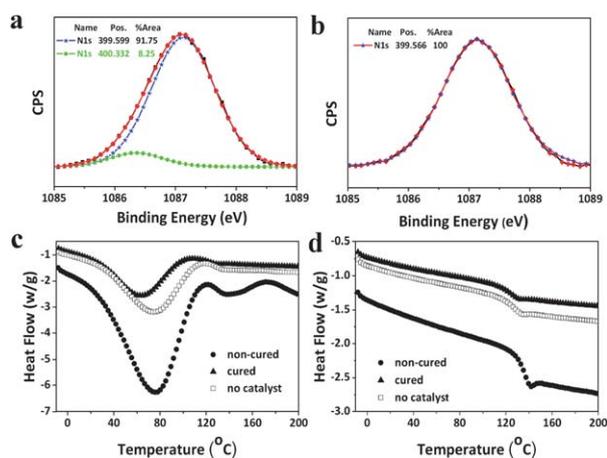
Fig. 4 High resolution N1s XPS spectra of electrospun PNIPAM/OpePOSS fibres and the curve-fitted peaks (a) after and (b) before curing treatment (PNIPAM : OpePOSS : EMI = 100 : 15 : 0.3, w/w). DSC curves of PNIPAM/OpePOSS nanofibres. (c) 1st and (d) 2nd heating scans. (the * mark indicates the temperature used for the curing treatment).

ethanol, and the contents of elements C, H, N and Si were then tested. Since OpePOSS and PNIPAM are both soluble in ethanol, such a leaching treatment should wash off all the un-reacted OpePOSS and linear PNIPAM. The elemental analyses of the same sample before and after heat and leaching treatments showed almost no difference (see ESI†). This confirms that almost all the chemical species present in the nanofibres participated in the crosslinking reaction, remaining immobilised within the network.

It should be mentioned that solid-state NMR was also tried, but failed to reveal any difference between the cured and non-cured nanofibre samples due to the broad peaks. Alternatively, a model reaction using OpePOSS, EMI and N-iso-propylacrylamide (the monomer of PNIPAM), was performed. The ¹³C-NMR spectra after the reaction showed two new peaks at 44.3 ppm and 71.6 ppm, respectively consistent with the formation of –C–N– bond and ring opening of epoxide (see ESI†).[20] For comparison, OpePOSS and N-iso-propylacrylamide were treated under the same condition. Without EMI, the peaks were almost unnoticeable in the spectrum, suggesting a low reaction yield.

Fig. 4c and d show the 1st and 2nd heating scans of the DSC curves for the PNIPAM/OpePOSS nanofibres. For all fibre samples, with or without EMI catalyst, the 1st heating scan revealed an endothermic peak at around 80–100 °C followed by a small exothermic crystallisation peak (110–120 °C). Compared with other two samples, such endothermic and the subsequent exothermic peaks for the cured sample were smaller. Thermogravimetric analysis (TGA) revealed a weight loss in the same temperature range (see ESI†). Therefore, for the cured nanofibres, the endothermic and post-exothermic peaks were assigned to the evaporation of moisture and the subsequent orientation of polymer segments within the crosslinked structure. For the non-cured samples, the endothermic and exothermic behavior was attributed to a combination of the moisture evaporation, thermal shrinkage and post-crystallisation. The DSC curve for the non-cured nanofibres containing EMI also showed an exothermic

Scheme 1 Reaction scheme for crosslinking of PNIPAM and OpePOSS using EMI as the catalyst.

peak at around 171 °C (onset 148 °C) (Fig. 4c), however no similar peak was found for the other samples. This indicates that crosslinking occurs in the non-cured nanofibres containing EMI, and the reaction is complete after the curing treatment. The crosslinking in the nanofibres which do not contain any EMI had very low efficiency. For the 2nd heating scan, the samples only showed a glass transition (T_g) peak at around 120–140 °C (Fig. 4d). It was also observed that a small exothermic peak appeared just after the T_g stage for the non-cured nanofibres containing the EMI catalyst. This could be attributed to the incomplete crosslinking reaction during the first heating scan. For the non-cured nanofibres without EMI, such an exothermic peak was very small.

These results verify that thermal crosslinking in the absence of the EMI catalyst has very low reaction rate and EMI plays a key role in accelerating the crosslinking reaction. This can also be used to explain why the nanofibre mat containing EMI did not shrink seriously during the curing treatment. When the fibre mat was directly placed into a 160 °C oven, it was heated instantly to a high temperature, triggering the crosslinking reaction. As a result of the fast formation of the crosslinked network, the mobility of the polymer chains was restricted considerably, therefore preventing the fibres from shrinking severely.

The LCST of the hydrogel fibres was measured and showed dependence on the OpePOSS composition. When PNIPAM contained 15% OpePOSS, the cured nanofibres had a LCST value of 31.8 °C. Increasing the OpePOSS content to 25% led to a slightly reduced LCST value, to about 31 °C (ESI†). In comparison, linear PNIPAM not containing any OpePOSS has a higher LCST value (34.1 °C). Such a small decrease in the LCST value due to crosslinking with OpePOSS can be attributed to the flexible propylglycidyl links between the OpePOSS and PNIPAM, therefore not restricting the configuration change of the N-isopropylacrylamide units during hydration/dehydration switches.

The influence of OpePOSS versus PNIPAM content on fibre diameter and swelling ratio was also examined. It was found that the presence of a small quantity of EMI allowed the preparation of non-dissolvable nanofibre mats for all OpePOSS/PNIPAM samples studied. The content in OpePOSS affected not only the resultant fibre diameter, but also the swelling ratio. With an increase in the concentration of OpePOSS from 0% to 30% (weight percentage based on PNIPAM), the average fibre diameter increased initially until the composition reached 15% and then decreased gradually. The average diameter of the nanofibres was measured to be around 700–800 nm (Fig. 5a).
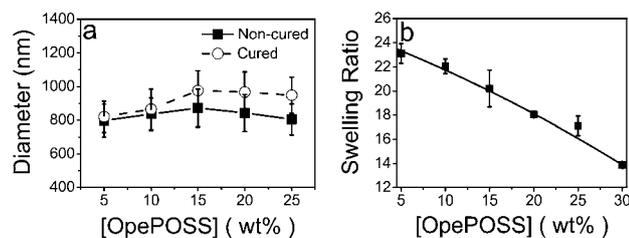
Also the swelling ratio of the nanofibre mats decreased with increasing the OpePOSS composition (Fig. 5b).

It was also interesting to find that the swollen PNIPAM nanofibre mat can be elongated up to 800% times of its original length without breaking (see ESI†). This ability could arise from two factors: the nanofibres progressively aligned along the direction of stretching, and the stretching induced a reduction of the fibre diameter to the advantage of their strength.

Conclusion

We have demonstrated a simple, novel but effective strategy to produce highly stable thermo-responsive PNIPAM hydrogel nanofibres by adding a POSS molecule with eight epoxide groups as crosslinker and a strong base catalyst to accelerate the crosslinking reaction. Insoluble nanofibres composed of a highly crosslinked PNIPAM polymer network were formed after electrospinning and subsequent curing treatment. The catalyst here plays a crucial role in the formation of a highly crosslinked polymer network and in maintaining the fibrous structure during the heat-curing treatment. The cured nanofibre mats can become swollen and transparent quickly upon contacting with water at a temperature below their lower critical solution temperature (LCST). The fibre mats responded quickly to changes in temperature, by shrinking and becoming opaque when exposed to water above the LCST, and by swelling and turning transparent again when exposed to water at temperature below their LCST. This smart behavior and their dimensional robustness in water make the produced hydrogel nanofibres highly valuable for applications in areas such as nano-actuators, sensors and "smart" biomedical tissue engineering scaffolds. The method of using OpePOSS and EMI to prepare highly crosslinked PNIPAM polymer network is also suitable for processing other hydrogel architectures.

Acknowledgements

References

1 A. K. Bajpai, S. K. Shukla, S. Bhanu and S. Kankane, *Prog. Polym. Sci.*, 2008, **33**, 1088–1118.

2 J. T. Zhang, S. W. Huang and R. X. Zhuo, *Macromol. Biosci.*, 2004, **4**, 575–578; C. M. Nolan, C. D. Reyes, J. D. Debord, A. J. Garcia and L. A. Lyon, *Biomacromolecules*, 2005, **6**, 2032–2039; C. L. Lo, K. M. Lin and G. H. Hsiue, *J. Controlled Release*, 2005, **104**, 477–488.

3 D. T. McQuade, A. E. Pullen and T. M. Swager, *Chem. Rev.*, 2000, **100**, 2537–2574; M. J. Serpe, C. D. Jones and L. A. Lyon, *Langmuir*, 2003, **19**, 8759–8764.

4 S. H. Gehrke, *Adv. Polym. Sci.*, 1993, **110**, 81–144; E. Kokufuta and K. Takahashi, *Polymer*, 1990, **31**, 1177–1182; T. Okano, Y. H. Bae, H. Jacobs and S. W. Kim, *J. Controlled Release*, 1990, **11**, 255–265.

5 X. Hu, G. Li, M. Li, J. Huang, Y. Li, Y. Gao and Y. Zhang, *Adv. Funct. Mater.*, 2008, **18**, 575–583.

6 J. M. Weissman, H. B. Sunkara, A. S. Tse and S. A. Asher, *Science*, 1996, **274**, 959–960; C. Wang, N. T. Flynn and R. Langer, *Adv. Mater.*, 2004, **16**, 1074–1079.

7 J. L. Drury and D. J. Mooney, *Biomaterials*, 2003, **24**, 4337–4351.

8 T. Nishikawa, K. Akiyoshi and J. Sunamoto, *J. Am. Chem. Soc.*, 1996, **118**, 6110–6115; D. Gan and L. A. Lyon, *J. Am. Chem. Soc.*, 2001, **123**, 8203–8209; T. Ito, T. Hioki, T. Yamaguchi, T. Shinbo, S. I. Nakao and S. Kimura, *J. Am. Chem. Soc.*, 2002, **124**,

Fig. 5 Influences of OpePOSS content (based on the weight of PNIPAM) on (a) fibre diameter and (b) swelling ratios of the cured PNIPAM/OpePOSS nanofibres. (OpePOSS : EMI = 100 : 2 w/w for all conditions.)

7840–7846; N. Liu, D. R. Dunphy, P. Atanassov, S. D. Bunge, Z. Chen, G. P. López, T. J. Boyle and C. J. Brinker, *Nano Lett.*, 2004, **4**, 551–554.

9 J. Fang, H. Niu, T. Lin and X. Wang, *Chin. Sci. Bull.*, 2008, **53**, 2265–2286.

10 M. Heskins and J. E. Guillet, *J. Macromol. Sci., Part A: Pure Appl. Chem.*, 1968, **A2**, 14; R. H. Pelton, H. M. Pelton, A. Morphesis and R. L. Rowell, *Langmuir*, 1989, **5**, 816–818.

11 D. N. Rockwood, D. B. Chase, R. E. Akins and J. F. Rabolt, *Polymer*, 2008, **49**, 4025–4032; H. Okuzaki, K. Kobayashi and H. Yan, *Synth. Met.*, 2009, **159**, 2273–2276; M. Chen, M. Dong, R. Havelund, V. R. Regina, R. L. Meyer, F. Besenbacher and P. Kingshott, *Chem. Mater.*, 2010, **22**, 4214–4221.

12 H. Okuzaki, K. Kobayashi and H. Yan, *Macromolecules*, 2009, **42**, 5916–5918.

13 R. París and I. Quijada-Garrido, *Polym. Int.*, 2009, **58**, 362–367.

14 P. Iyer, J. A. Mapkar and M. R. Coleman, *Nanotechnology*, 2009, **20**, 325603; T. Ceyhan, M. Yuksek, H. G. Yaglioglu, B. Salih, M. K. Erbil, A. Elmali and O. Bekaroglu, *Dalton Trans.*, 2008, 2407–2413; C. Wan, F. Zhao, X. Bao, B. Kandasubramanian and M. Duggan, *J. Phys. Chem. B*, 2008, **112**, 11915–11922; J. Mu and S. Zheng, *J. Colloid Interface Sci.*, 2007, **307**, 377–385.

15 T. Lin, H. Wang, H. Wang and X. Wang, *Nanotechnology*, 2004, **15**, 1375–1381.

16 C. Tang, S. Ye and H. Liu, *Polymer*, 2007, **48**, 4482–4491.

17 J. F. Mu and S. X. Zheng, *J. Colloid Interface Sci.*, 2007, **307**, 377–385.

18 H. A. Staab, *Angew. Chem., Int. Ed. Engl.*, 1962, **1**, 351–367.

19 F. Zhang and M. P. Srinivasan, *Colloids Surf., A*, 2005, **257–258**, 295–299.

20 E. Buravlev, I. Chukicheva and A. Kuchin, *Chem. Nat. Compd.*, 2010, **46**, 33–35.